Quantitative determination of domain distribution in $SrTiO_3$—competing effects of applied electric field and mechanical stress

2010 J. Phys.: Condens. Matter 22 235903

(http://iopscience.iop.org/0953-8984/22/23/235903)

J. Phys.: Condens. Matter **22** (2010) 235903 (8pp) doi:10.1088/0953-8984/22/23/235903

Quantitative determination of domain distribution in $SrTiO_3$—competing effects of applied electric field and mechanical stress

J Sidoruk[1], J Leist[1], H Gibhardt[1], M Meven[2], K Hradil[1] and G Eckold[1]

[1] Institut für Physikalische Chemie, Georg August Universität Göttingen, Germany
[2] Institut für Kristallographie, RWTH Aachen and FRM-II, Garching, Germany

Received 1 April 2010, in final form 3 May 2010
Published 21 May 2010
Online at stacks.iop.org/JPhysCM/22/235903

Abstract
Below its ordering temperature at 105 K, perovskite-type $SrTiO_3$ exhibits a tetragonal phase with three different structural domains that are strongly influenced by the application of uniaxial mechanical stresses and electric fields. A careful neutron diffraction study of superlattice reflections provides full quantitative information about the varying domain distributions under external loads as a function of temperature. It is shown that electric field and uniaxial stress exhibit competitive effects and the simultaneous application leads to a complex redistribution behaviour of the tetragonal domains. The results are discussed in the context of the formation of a field induced ferroelectric phase at low temperatures. The experimental findings demonstrate that its polarization is always perpendicular to the tetragonal axis and the polar phase has orthorhombic symmetry.

1. Introduction

Strontium titanate ($SrTiO_3$) is a well known member of the perovskite family. Due to its structural properties, it is widely used in multilayer ferroelectric thin films [1] and as a substrate for high temperature superconductors [2]. Moreover it is a famous example of a crystal undergoing a displacive phase transition. Cooling below $T_C = 105$ K leads to a tetragonal distorted phase with the space group $I4/mcm$ [3]. This antiferrodistortive transition is associated with an antiphase rotation of adjacent titanate octahedra about one of the main axes of the cubic parent structure. This transformation is induced by the condensation of a softmode at the R-point of the Brillouin zone [4, 5]. Unlike the isostructural barium compound, $SrTiO_3$ does not become ferroelectric even at the lowest temperatures, since the competing polar mode at the Γ-point shows only an incomplete softening and remains at a non-zero frequency [6]. The suppression of the ferroelectric phase transition is attributed to the zero point motion of this low-frequency Γ-point mode that prevents the formation of an ordered structure. Rather, a so-called quantum paraelectric state [7] is observed that is characterized by a large dielectric constant reflecting the existence of dipole fluctuations instead of long range ferroelectric order. Due to the delicate equilibrium of forces it is possible to induce ferroelectricity by applying an additional external driving force such as mechanical stress [8] or electric field [9] at sufficiently low temperatures.

During the antiferrodistortive phase transition, three types of tetragonal domains are formed since the symmetry axis can be oriented along each of the three cubic principal axes. Hence, bulk crystals usually exhibit a multi-domain state below T_c. This is known to be the source of anomalies at low temperatures like additional lines in the excitation spectrum or changes in the sound velocity [10]. Usually, it is assumed that all tetragonal domains are equally distributed even if there are indications that the growth direction of the crystal already induces a preferred orientation [10].

It was observed that the application of uniaxial mechanical stress can change the domain distribution appreciably [11, 12]. Since the tetragonal distortion corresponds to a c/a-ratio slightly larger than unity [13], stress along the [110]-direction results in a preference for domains with a tetragonal axis along [001]. Stresses of the order 20 MPa are already sufficient

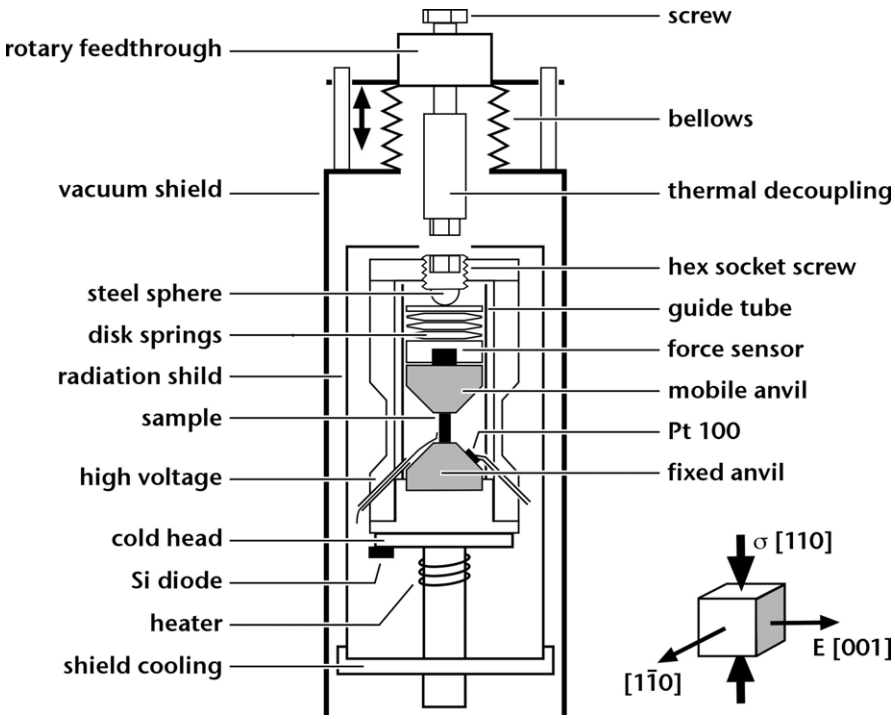

Figure 1. Pressure cell for a closed cycle cryostat. The inset shows the orientation of the sample with respect to the applied stress and electric field.

to obtain almost monodomain samples. This is an order of magnitude smaller than the critical stress needed to induce ferroelectricity [8].

While previous publications concentrated on the influence of mechanical stress, we recently reported that the intensities of superlattice reflections and thus the domain volumes are strongly affected by an external electric field [14]. Although a direct coupling between the antiferrodistortive order parameter and the electric field is forbidden by symmetry, a clear indication of domain redistribution was observed. While indications of such behaviour were mentioned even in the 1970s [15, 16], to the best of our knowledge a thorough investigation has not been performed so far.

In this contribution, we present a systematic study of the domain distribution under pressure, electric field and a combination of both quantities. It will be shown that electric fields and uniaxial stresses exhibit competing effects excluding the formation of a monodomain ferroelectric state.

Note, that throughout this paper we will use cubic indices for all reflections, even in the tetragonal phase, neglecting the small tetragonal distortion.

2. Experimental details

Neutron scattering experiments have been performed at the hot neutron diffractometer HEIDI at the FRM II neutron source in Garching [17] using a wavelength of 0.87 Å. Some additional data have been obtained at the triple axis spectrometer PUMA [18]. A pressure cell was constructed to be used with a closed cycle cryostat that can be mounted in the Eulerian cradle of the diffractometer. Figure 1 shows a schematic drawing of the cell that enabled us to apply a maximal force of 2 kN and simultaneously an electric field of several kV cm^{-1}. To minimize scattering from the sample environment all components of the cell located close to the neutron beam are made of aluminium or aluminium oxide (in the case of the bevelled anvils).

The [110]-face of the sample is attached to the fixed anvil using an epoxy resin adhesive. All mobile components are located in a guide tube to prevent canting. Above the mobile anvil a miniature force sensor produced by Burster GmbH is used to measure the applied stress. The disk springs that transmit the force can be pressed by turning a hexagonal socket screw with an integrated steel sphere. Thermal decoupling is achieved by using the polymer material Vespel® SP1 (DuPont™) with a low thermal conductivity to operate this screw from outside the cryostat with a rotary feedthrough. At low temperatures, this connection can be withdrawn from the screw to prevent heat leakage. The temperature is monitored with a Pt100 resistor attached directly to the fixed anvil in the vicinity of the sample. An additional Si-diode is located at the cold head of the cryostat. The long term stability of the system is better than 0.1 K.

Samples of high quality were cut from a commercial $SrTiO_3$-boule provided by MaTecK GmbH. In order to prevent formation of additional dislocations we refrained from polishing the sample faces. Typical sizes of the transparent and colourless specimen were about $4 \times 6 \times 8$ mm^3. The mosaicity was determined with high resolution γ-diffraction using 316 keV radiation from an Ir-192 source and was below 0.03°. Electrodes were applied to the [001]-face of the sample with silver paint.

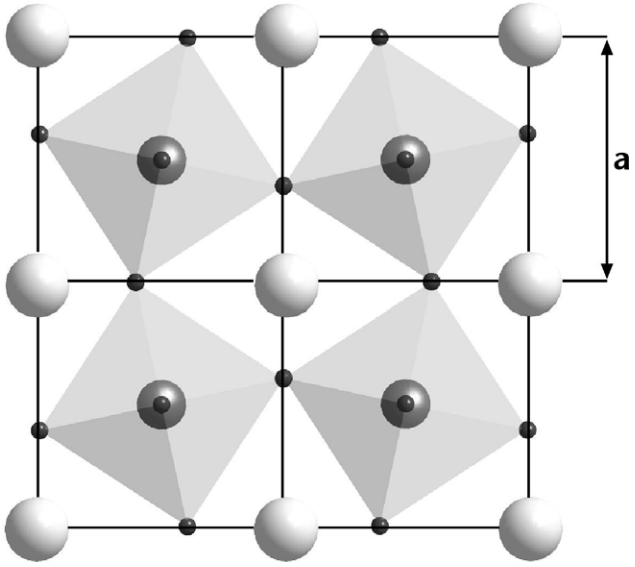

Figure 2. Projection along [001] of the supercell used to describe the structure factors of superlattice reflections. Within each second plane, the rotation of the TiO_6-octahedra is in the opposite direction.

The integrated intensities of 15 superlattice reflections (SLR) were determined from ω-scans close to the bisection position to minimize absorption by the anvils. The background was determined by the extended Lehmann–Larsen algorithm after applying the usual Lorentz correction. The intensities were corrected for thermal diffuse scattering using the residual intensity at the SLR-position above the phase transition at 105 K.

3. Data evaluation

In the following, we restrict ourselves to the discussion of superlattice reflections of the tetragonal phase of $SrTiO_3$ that is stable below 105 K. Using the cubic notation, these SLRs are characterized by half-integer Miller indices (h k l). If the tetragonal axis is along the z-direction (z-domain) the structure factor of an SLR is given by the displacements of oxygen atoms within the x–y-plane. Since adjacent TiO_6-octahedra are always rotated in the opposite sense, the structure factor can be calculated as a sum of phase factors of oxygen atoms in an eight-fold supercell as indicated in figure 2.

$$F_{hkl}^{(z)} = \sum_{n=1}^{16} \mathrm{e}^{\mathrm{i}2\pi[h(x_n+u_{x,n})+k(y_n+u_{y,n})+lz_n]}. \qquad (1)$$

Note that this supercell is twice the size of the tetragonal primitive cell. Since we are using the cubic notation, this approach is adequate. The scattering lengths and the Debye–Waller factors are omitted since, in the following, we will consider only ratios of structure factors. In table 1, the displacements (u_x, u_y, u_z) of the individual oxygen atoms located at (x, y, z) are listed.

For the other x- and y-domains corresponding structure factors $F_{hkl}^{(x)}$ and $F_{hkl}^{(y)}$ are obtained. The total intensity of an SLR is given by

$$I_{hkl} \propto V_x|F_{hkl}^{(x)}|^2 + V_y|F_{hkl}^{(y)}|^2 + V_z|F_{hkl}^{(z)}|^2 \qquad (2)$$

where the V_is are the volumes of the respective domains. It is easily seen that according to table 1 for SLRs of the type (hkk), (hkh) and (hhl), there is no contribution of the x, y and z-domains, respectively. Hence the volume fraction of each domain

$$\phi_i = \frac{V_i}{V_x + V_y + V_z} \qquad (3)$$

can be calculated from any set of three SLRs like $(\frac{7}{2}\ \frac{1}{2}\ \frac{1}{2})$, $(\frac{1}{2}\ \frac{7}{2}\ \frac{1}{2})$ and $(\frac{1}{2}\ \frac{1}{2}\ \frac{7}{2})$. We have carefully determined the integrated intensities of the set of SLRs listed in table 2. Different approaches have been applied to determine the volume fractions of the three domains: on the one hand, the volume fractions were directly calculated from each of the groups of reflections (1–3), (4–6), (13–15). The full set of SLR-intensities, on the other hand, was used for a fit by the volume fractions according to equation (2). All methods of evaluation yielded consistent results, proving the high quality of the data.

Table 1. Displacements u of oxygen atoms in a tetragonal z-domain in units of the cubic lattice parameter a.

Atom	x	y	z	u_x	u_y	u_z
O_1	$\frac{1}{2}$	0	$\frac{1}{2}$	$-u$	0	0
O_2	$\frac{3}{2}$	0	$\frac{1}{2}$	u	0	0
O_3	0	$\frac{1}{2}$	$\frac{1}{2}$	0	u	0
O_4	1	$\frac{1}{2}$	$\frac{1}{2}$	0	$-u$	0
O_5	$\frac{1}{2}$	1	$\frac{1}{2}$	u	0	0
O_6	$\frac{3}{2}$	1	$\frac{1}{2}$	$-u$	0	0
O_7	0	$\frac{3}{2}$	$\frac{1}{2}$	0	$-u$	0
O_8	1	$\frac{3}{2}$	$\frac{1}{2}$	0	u	0
O_9	$\frac{1}{2}$	0	$\frac{3}{2}$	u	0	0
O_{10}	$\frac{3}{2}$	0	$\frac{3}{2}$	$-u$	0	0
O_{11}	0	$\frac{1}{2}$	$\frac{3}{2}$	0	$-u$	0
O_{12}	1	$\frac{1}{2}$	$\frac{3}{2}$	0	u	0
O_{13}	$\frac{1}{2}$	1	$\frac{3}{2}$	$-u$	0	0
O_{14}	$\frac{3}{2}$	1	$\frac{3}{2}$	u	0	0
O_{15}	0	$\frac{3}{2}$	$\frac{3}{2}$	0	u	0
O_{16}	1	$\frac{3}{2}$	$\frac{3}{2}$	0	$-u$	0

4. Results

In figure 3, raw data of the set of SLRs 1–3 are shown for the reference state of the sample before applying mechanical stress or an electric field (top), under a load of 16 MPa (middle) and under the influence of an electric field of 9.2 kV cm^{-1}.

If all three domains had equal volume fractions, the intensities of the three reflections would be identical. It is easily seen that even in the reference sample, the $(\frac{1}{2}\ -\frac{1}{2}\ \frac{7}{2})$-reflection is considerably weaker than the others, giving evidence that the z-domain is favoured. This preference might

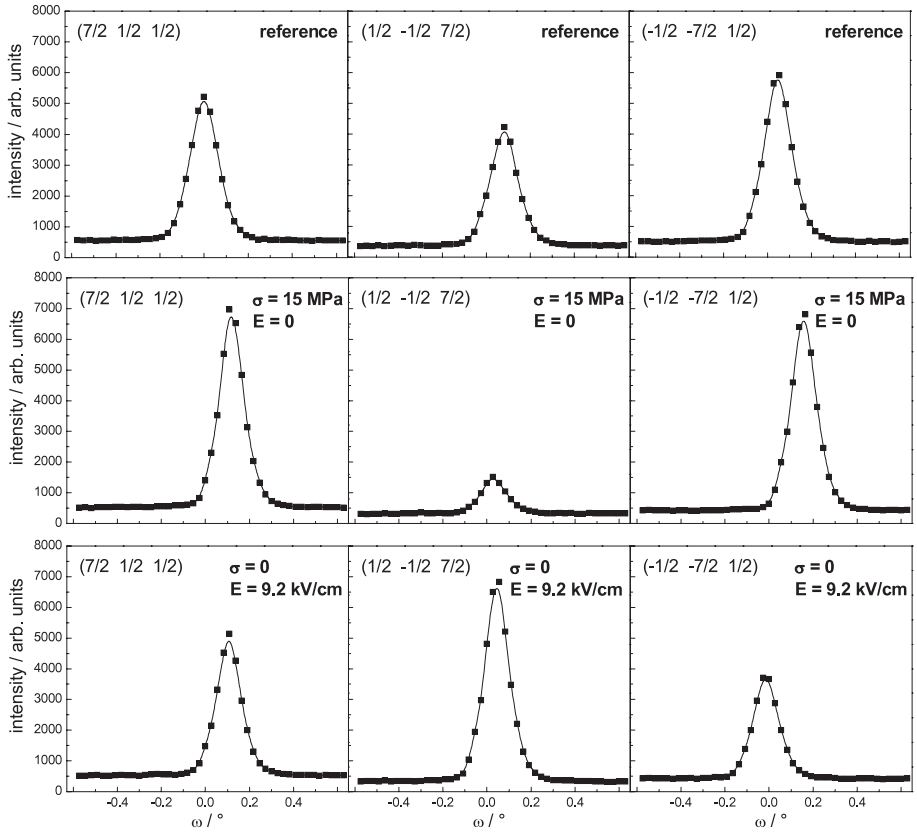

Figure 3. Intensity profiles of SLRs 1–3 for the reference state of the crystal (top), under mechanical stress of 15 MPa (middle) and an electric field of 9.2 kV cm^{-1} (bottom). Note that the slight variation of the peak position is due to the limited accuracy of the orientation matrix for the relatively large sample.

Table 2. List of measured superlattice reflections (SLRs).

	$(h\ k\ l)$
1	$(\frac{7}{2}\ \frac{1}{2}\ \frac{1}{2})$
2	$(\frac{1}{2}\ -\frac{1}{2}\ \frac{7}{2})$
3	$(-\frac{1}{2}\ -\frac{7}{2}\ \frac{1}{2})$
4	$(\frac{1}{2}\ \frac{7}{2}\ \frac{7}{2})$
5	$(\frac{7}{2}\ \frac{1}{2}\ \frac{7}{2})$
6	$(\frac{7}{2}\ \frac{7}{2}\ \frac{1}{2})$
7	$(\frac{5}{2}\ \frac{3}{2}\ \frac{1}{2})$
8	$(\frac{3}{2}\ \frac{1}{2}\ \frac{5}{2})$
9	$(-\frac{1}{2}\ -\frac{5}{2}\ \frac{3}{2})$
10	$(-\frac{5}{2}\ -\frac{7}{2}\ \frac{3}{2})$
11	$(\frac{3}{2}\ \frac{5}{2}\ \frac{7}{2})$
12	$(\frac{7}{2}\ \frac{3}{2}\ \frac{5}{2})$
13	$(\frac{3}{2}\ \frac{1}{2}\ \frac{1}{2})$
14	$(\frac{1}{2}\ \frac{3}{2}\ \frac{1}{2})$
15	$(\frac{1}{2}\ \frac{1}{2}\ \frac{3}{2})$

be due to the preparation since the z-direction is the growth direction of the $SrTiO_3$-boule from which the sample was cut. Applying pressure along [110] strongly enhances this tendency. An electric field along [001], however, has an almost opposite effect.

In order to determine a possible memory effect, a sequence of experiments at different temperatures, stresses and electric fields was performed. The corresponding domain volume fractions are tabulated in table 3.

The results of runs 1 and 12 at 120 K (above T_c) were used to estimate the background intensity due to thermal diffuse scattering. According to the temperature dependence of the softmode, a considerable variation of the thermal diffuse scattering is to be expected. Nevertheless, the correction for the integrated intensities is rather small and the possible errors are considered in table 3. An exception is the very weak SLR-type (113), where larger discrepancies are observed.

In order to start each cooling sequence from almost equivalent initial states, the sample was heated to 120 K after runs 4, 7, 16 and 22, respectively.

Inspection of table 3 yields the following results:

(1) The reference sample consists of almost 50% z-domains.
(2) Stress of 5 MPa leads to an increase of z-domains of more than 30%, while 15 MPa results in almost complete suppression of x- and y-domains.
(3) Without applied electric field, the domain distribution is almost independent of temperature.
(4) The domain distribution remains almost unchanged if the stress is removed. Even heating to 120 K is not sufficient to destroy the memory of the sample, as seen by the results of runs 13–15. Hence, external stress exhibits irreversible effects on the domain distribution.

Table 3. Volume fractions of the tetragonal domains under different conditions in chronological order.

Run	T (K)	σ (MPa)	E (kV cm^{-1})	ϕ_x (%)	ϕ_y (%)	ϕ_z (%)
1	120					
2	80			24.9 ± 5.5	26.4 ± 5.4	48.7 ± 6.8
3	50			29.3 ± 6.8	23.7 ± 5.7	47.0 ± 7.7
4	20			30.9 ± 7.5	23.0 ± 6.1	46.1 ± 8.3
5	80	5		6.3 ± 3.8	12.1 ± 4.6	81.6 ± 6.4
6	50	5		5.7 ± 4.3	10.0 ± 5.0	84.3 ± 7.2
7	20	5		6.0 ± 4.0	9.8 ± 4.3	84.2 ± 6.4
8	80		4.6	14 ± 3.1	30.3 ± 3.9	55.7 ± 4.6
9	50		4.6	18.6 ± 4.7	43.1 ± 7.1	38.3 ± 7.1
10	20		4.6	36.4 ± 7.6	57.9 ± 8.0	5.7 ± 2.9
11	20			3.6 ± 2.9	18.8 ± 4.7	77.6 ± 5.6
12	120					
13	80			4.5 ± 2.9	11.4 ± 3.2	84.1 ± 4.4
14	50			3.7 ± 2.6	11.0 ± 3.0	85.3 ± 4.0
15	20			3.8 ± 2.6	10.9 ± 3.0	85.3 ± 4.0
16	20		4.6	34.3 ± 8.5	59.4 ± 9.1	6.3 ± 3.2
17	80	15		1.4 ± 2.5	6.8 ± 2.5	91.8 ± 3.5
18	50	15		3.6 ± 2.7	5.9 ± 2.5	90.5 ± 3.7
19	20	15		3.7 ± 2.6	6.4 ± 2.4	89.9 ± 3.6
20	20	15	4.6	18.4 ± 4.1	12.0 ± 2.8	69.6 ± 5.0
21	20	15	9.2	38.4 ± 4.8	18.4 ± 3.3	43.2 ± 4.8
22	20	15		3.8 ± 2.9	6.3 ± 2.7	89.9 ± 4.1
23	80		9.2	22.4 ± 3.5	40.5 ± 4.4	37.1 ± 4.4
24	50		9.2	35.4 ± 7.3	55.6 ± 7.8	9.0 ± 3.5
25	20		9.2	39.4 ± 8.4	54.1 ± 8.8	6.5 ± 3.1

(5) An applied electric field, on the other hand, shows entirely reversible effects even at 20 K (runs 10 and 11).
(6) The electric field along [001] leads to a temperature dependent redistribution of domains, where the z-domains are transformed into x- and y-domains with a slight preference of y-domains. This effect becomes stronger if the temperature is decreased (runs 8–10 and 23–25) and the induced ferroelectric phase is approached.
(7) At 80 K and 4.6 kV cm^{-1} (run 8), there are 55% z-domains left, while at 20 K, these domains disappear almost completely. Doubling the electric field leads to the suppression of z-domains even at 50 K.
(8) Simultaneous application of stress and field hinders the redistribution as can be seen from runs 19 to 22. Under 15 MPa, we have about 90% z-domains that are reduced reversibly to 43% by an electric field of 9.2 kV cm^{-1} (run 21). Interestingly, in contrast to the stress-free behaviour now the x-domain is somewhat favoured over the y-domain.

5. Discussion

Preferred orientations of tetragonal domains in $SrTiO_3$ even without any external perturbation have already been observed by Müller *et al* [11] in thin wafers and by Arzel *et al* [10] in bulk crystals along the growth direction. Either the defect structure due to the growth process or the introduction of strains during the preparation of the samples seems to be the origin of the preference of a single domain.

The tetragonal distortion below T_c is the reason for the domain redistribution under mechanical stress as already pointed out by Müller *et al* [11] and Chang *et al* [12]. In good agreement with the results of these authors, we found that uniaxial stress along [110] leads to the formation of an almost monodomain sample. This redistribution is irreversible. Even after the crystal is heated into the cubic phase and the stress is released, almost the same domain distribution is recovered on subsequent cooling. This finding seems to be somewhat different to observations of Chang *et al* [12]. Careful re-inspection of the mosaic structure of the sample by high resolution γ-diffraction has proven a small irreversible modification of the dislocation structure, i.e. a slight broadening of the mosaic distribution ($\sim$0.05°). This indicates that some residual stresses are present in the sample that may be responsible for the observed memory effect.

At first sight, the strong effect of an applied electric field on the tetragonal domain structure is unexpected and surprising. Due to the different symmetries of the order parameter η and the electric field-vector, no linear coupling is possible. The Landau-expansion of the free energy has been formulated by Slonczewski and Thomas [19] and Cowley [20] as a function of order parameter and elastic strains. Sakudo and Unoki [21] have considered the coupling to the electrical polarization where the leading term is quadratic in polarization or electric field.

Even if the critical behaviour of $SrTiO_3$ is not correctly described by the simple Landau-expansion, it is nevertheless worthwhile to consider it as a basis for the qualitative interpretation of the possible influence of electric fields and mechanical stresses. If we extend this expansion to take into account possible field effects, we arrive at the following expression for the free energy density:

$$
\begin{aligned}
G = {} & A_1(T - T_{c1})(\eta_x^2 + \eta_y^2 + \eta_z^2) + A_2(\eta_x^4 + \eta_y^4 + \eta_z^4) \\
& + A_3(T - T_{c2})P_z^2 + A_4 P_z^4 + A_5(\varepsilon_{xx} + \varepsilon_{yy} + \varepsilon_{zz}) \\
& + A_6(\varepsilon_{xx}^2 + \varepsilon_{yy}^2 + \varepsilon_{zz}^2) + A_7(\varepsilon_{xx}\varepsilon_{yy} + \varepsilon_{xx}\varepsilon_{zz} + \varepsilon_{yy}\varepsilon_{zz}) \\
& + A_8(\eta_x^2 + \eta_y^2)P_z^2 + A_9\eta_z^2 P_z^2 \\
& + A_{10}(\eta_x^2\varepsilon_{xx} + \eta_y^2\varepsilon_{yy} + \eta_z^2\varepsilon_{zz}) \\
& + A_{11}(\eta_x^2 + \eta_y^2 + \eta_z^2)(\varepsilon_{xx} + \varepsilon_{yy} + \varepsilon_{zz}) \\
& + A_{12}P_z^2(\varepsilon_{xx} + \varepsilon_{yy}) + A_{13}P_z^2\varepsilon_{zz} \\
& + [-1 + A_{14}(\eta_x^2 + \eta_y^2) + A_{15}(\varepsilon_{xx} + \varepsilon_{yy}) + A_{16}\eta_z^2 \\
& + A_{17}P_z^2 + A_{18}\varepsilon_{zz}]P_z E_z + [A_{19}(\eta_x^2 + \eta_y^2) \\
& + A_{20}(\varepsilon_{xx} + \varepsilon_{yy}) + A_{21}\eta_z^2 + A_{22}P_z^2 + A_{23}\varepsilon_{zz}]E_z^2 \\
& + A_{24}\varepsilon_{zz}\sigma_0 + A_{25}(\varepsilon_{xx} + \varepsilon_{yy})\sigma_0 \\
& + [A_{26}(\eta_x^2 + \eta_y^2) + A_{27}\eta_z^2 + A_{28}P_z^2]\sigma_0. \qquad (4)
\end{aligned}
$$

Here, (η_x, η_y, η_z) is the three-dimensional order parameter, $(\varepsilon_{xx}, \varepsilon_{yy}, \varepsilon_{zz})$ are the three longitudinal strain components, P_z is the induced electric polarization along the applied electric field E_z and σ_0 is the mechanical stress along [110]. This expansion is restricted to fourth order in ϕ and second order in E_z. Moreover, shear strains as well as products of different components of the order parameter are neglected since these are only expected close to domain boundaries. As usual, the temperature dependence of the free energy is described by the prefactors of the quadratic terms of order parameter and polarization, and all expansion coefficients are regarded as temperature independent. T_{c1} marks the transition into the tetragonal phase and T_{c2} is used to describe the proximity of the ferroelectric phase.

Minimization of the free energy allows one to determine order parameter, strain components as well as polarization as a function of applied field and stress. Far from the ferroelectric transition, the induced polarization can be written as

$$P_z = \frac{B_0 + B_1\sigma_0}{B_2 + B_3\sigma_0}E_z = \chi_{el}E_z. \qquad (5)$$

The coefficients B_i are some combinations of the expansion coefficients of the free energy density. B_0 is temperature dependent and so is the electric susceptibility χ_{el}.

For the order parameter components we obtain within the tetragonal phase

$$\eta_x = \eta_y = \sqrt{C_0 + (C_1\chi_{el}^2 + C_2\chi_{el} + C_3)E_z^2 + C_4\sigma_0} \qquad (6)$$

$$\eta_z = \sqrt{C_0 + (C_5\chi_{el}^2 + C_6\chi_{el} + C_7)E_z^2 + C_8\sigma_0}. \qquad (7)$$

Thus, the ratio of domain volumes equates to

$$\frac{\phi_z}{\phi_x} = \frac{\phi_z}{\phi_y} = \sqrt{\frac{C_0 + (C_5\chi_{el}^2 + C_6\chi_{el} + C_7)E_z^2 + C_8\sigma_0}{C_0 + (C_1\chi_{el}^2 + C_2\chi_{el} + C_3)E_z^2 + C_4\sigma_0}}. \qquad (8)$$

Only if E_z or σ_0 are non-zero, the volume fractions of the domains ϕ_x and ϕ_y, on the one hand, and ϕ_z, on the other hand, become different. For small external perturbations, the domain redistribution is proportional to the square of the applied field while it is directly proportional to mechanical strains. The

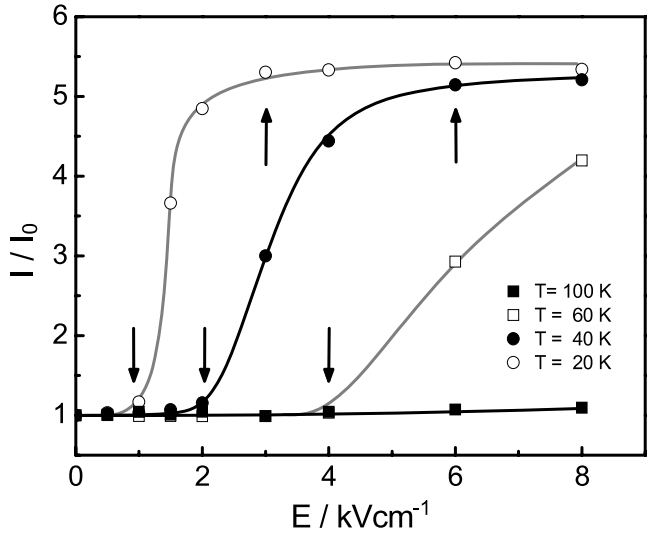

Figure 4. Field dependence of the $(\frac{1}{2}\ \frac{1}{2}\ \frac{3}{2})$ SLR intensity at different temperatures (PUMA-data), lines are a guide to the eye.

experimental findings (E_z favouring ϕ_x and ϕ_y, σ_0 favouring ϕ_z) require:

$$\begin{aligned} C_5\chi_{el}^2 + C_6\chi_{el} + C_7 < 0 \qquad & C_1\chi_{el}^2 + C_2\chi_{el} + C_3 > 0 \\ C_8 > 0 \qquad & C_4 < 0. \end{aligned} \qquad (9)$$

Moreover, the electric field effect is temperature dependent due to the variation of the susceptibility. In contrast, the influence of mechanical stress should be almost temperature independent. This is just what is found experimentally.

The present results show that the coupling of the order parameter to the electric field is sufficiently strong to allow for a drastic redistribution of tetragonal domains. By the application of several kV cm^{-1} it is even possible to overcompensate the effect of moderate stress and switch the domain state completely from z to x/y. This finding is consistent with the results of Schmidt and Hegenbarth [22] who obtained an electrostrictive deformation of the order 10^{-6} at 80 K and $E = 4.6$ kV cm^{-1}—a quantity that can equally well be produced by applied stresses of some 10 MPa.

In view of the present results, the main source of deformation seems to be the domain redistribution due to the c/a-tetragonal ratio rather than a true piezoelectric effect. Alefeld has determined this ratio with extremely good accuracy to be of the order $1 + 10^{-5}$ [13]. The deviation from unity is comparable with the deformation ε_3 that may be estimated from the apparent piezoelectric coefficient d_{31} obtained by Schmidt *et al* [22] ($\varepsilon_3 \approx 2 \times 10^{-5}$ at 10 kV cm^{-1} and 20 K). The present interpretation is also consistent with the findings of Grupp and Goldmann [23] who observed a quadratic field dependence of the strain within the tetragonal phase that becomes linear as soon as the field induced ferroelectric phase is entered. This behaviour is generally accepted [24], even if there are some doubts about the interpretation of the original data of Grupp and Goldmann [25].

The field dependence of the domain redistribution may be characterized by the intensity of the SLR $(\frac{1}{2}\ \frac{1}{2}\ \frac{3}{2})$ as

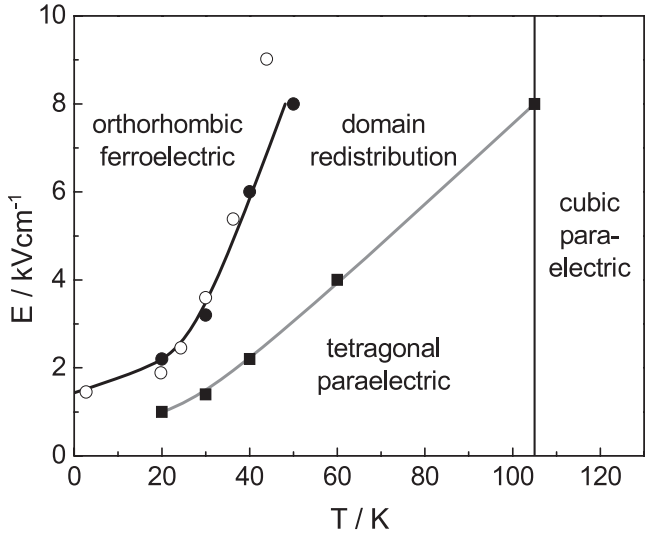

Figure 5. Temperature dependence of the critical fields: squares and full circles correspond to the threshold and saturation fields, i.e. down and up arrows in figure 4, respectively. Open symbols characterize the phase transition into the ferroelectric phase according to the dielectric data of Hegenbarth [26].

shown in figure 4. Obviously, there is some threshold field (down arrows) for the redistribution. Moreover, a saturation of the intensity at high fields is observed (up arrows) that corresponds to a complete redistribution. The temperature dependence of the corresponding critical fields is shown in figure 5. At low fields and high enough temperatures, we find the normal tetragonal paraelectric behaviour. Domain redistribution is observed within the E–T-regime limited by the two lines. Interestingly, the transition into the ferroelectric field induced phase coincides with the completion of the redistribution as shown by comparison with the dielectric data of Hegenbarth [26].

Itoh *et al* [27] observed in isotope enriched $SrTi^{18}O_3$ the ferroelectric phase even at zero field; it is not suppressed by quantum fluctuations. In this system, Dec *et al* [28] have found similar results for the domain redistribution with an almost linear temperature dependence of the threshold field. Due to the presence of the ferroelectric phase, however, considerably smaller fields are required.

It is believed that the anisotropy of the dielectric susceptibility along with the large electrostrictive coefficient is the main reason for the preference of domains with their tetragonal axis perpendicular to the applied electric field. As a simple illustration, figure 6 shows that the top oxygen ions are likely to be displaced in a direction perpendicular to the field induced shift of the titanium-ion along z. Hence, the x- and y-domains are favoured as observed experimentally.

The present results show that it is in principle impossible to retain a monodomain sample both under stress along [110] and electric field along [001]. A single domain state of the tetragonal phase can only be expected if both are applied along the same [110]-direction. In any case, the polarization of the induced ferroelectric phase is perpendicular to the tetragonal axis. Hence, the polar phase always exhibits orthorhombic symmetry of space group $P2mm$.

6. Conclusion

By careful neutron diffraction experiments, we have studied quantitatively the domain distribution in $SrTiO_3$ as a function of temperature, uniaxial stress and electric field. It is found that electric field and stress exhibit competitive effects on the domain structure below the antiferrodistortive phase transition at 105 K, while stress along [110] is able to produce monodomain samples with their tetragonal axis along [001]. The application of an electric field along [001] leads to a reorientation of the symmetry axis towards [100] or [010] and hence again to a multi-domain state. At sufficiently low temperatures and/or large electric fields, the original domain can even be completely suppressed before finally the field induced ferroelectric phase is entered. These results show that it is impossible to obtain a single domain polar state of $SrTiO_3$ with polarization along one of the cubic axes.

References

[1] Jayadevan K P and Tseng T Y 2002 *J. Mater. Sci., Mater. Electron.* **13** 439
[2] Sum R, Lang H P and Güntherodt H-J 1995 *Physica* C **242** 174
[3] Unoki H and Sakudo T 1967 *J. Phys. Soc. Japan* **23** 546
[4] Shirane G and Yamada Y 1969 *Phys. Rev.* B **177** 858
[5] Cowley R A, Buyers W J L and Dolling G 1969 *Solid State Commun.* **7** 181
[6] Yamada Y and Shirane G 1969 *J. Phys. Soc. Japan* **26** 396
[7] Müller K A and Burkard H 1979 *Phys. Rev.* B **19** 3593
[8] Fujii Y, Uwe H and Sakudo T 1987 *J. Phys. Soc. Japan* **56** 1940

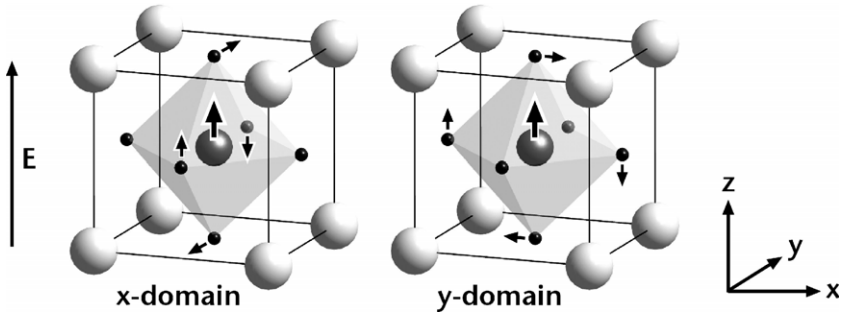

Figure 6. Model for the domain redistribution. The displacement of the Ti^{4+}-ion in the centre of the octahedron in the direction of the electric field leads to a preferred formation of x- and y-domains.

[9] Hemberger J *et al* 1996 *J. Phys.: Condens. Matter* **8** 4673
[10] Arzel L, Hehlen B, Currat R, Hennion B, Saint-Paul M and Courtens E 2000 *Ferroelectrics* **236** 81
[11] Müller K A, Berlinger W, Capizzi M and Gränicher H 1970 *Solid State Commun.* **8** 549
[12] Chang T S 1972 *J. Appl. Phys.* **43** 3591
[13] Alefeld B 1969 *Z. Phys.* **222** 155
[14] Leist J, Sidoruk J, Gibhardt H, Hradil K, Meven M and Eckold G 2010 *Diffus. Fundam.* at press
[15] Pietrass B 1972 *Phys. Status Solidi* a **9** K39
[16] Unoki H and Sakudo T 1973 *J. Phys. Soc. Japan* **35** 1128
[17] Hutanu V, Meven M and Heger G 2007 *Physica* B **397** 135
[18] Link P, Eckold G and Neuhaus J 2000 *Physica* B **276–278** 122
[19] Slonczewski J C and Thomas H 1970 *Phys. Rev.* B **1** 3599
[20] Cowley R 1996 *Phil. Trans. R. Soc.* **354** 2799
[21] Sakudo T and Unoki H 1971 *Phys. Rev. Lett.* **26** 851
[22] Schmidt G and Hegenbarth E 1963 *Phys. Status Solidi* **3** 329
[23] Grupp D E and Goldmann A M 1997 *Phys. Rev. Lett.* **78** 3511
[24] Maglione M 1998 *Phys. Rev. Lett.* **81** 3299
[25] Grupp D E and Goldmann A M 1999 *Phys. Rev. Lett.* **82** 3001
[26] Hegenbarth E 1964 *Phys. Status Solidi* **6** 333
[27] Itoh M, Wang R, Inaguma Y, Yamaguchi T, Shan Y J and Nakamura T 1999 *Phys. Rev. Lett.* **82** 3540
[28] Dec J, Kleemann W, Boldyreva K and Itoh M 2005 *Ferroelectrics* **314** 7